Network pharmacology-based approach reveals that Fructus mume exerts therapeutic effects against ulcerative colitis via the AGE/RAGE signaling pathway

Rui Wang [a,b,c], Xingchen Wang [c], Jinmei Ou [a,d,e,*]

[a] *Anhui University of Chinese Medicine, Hefei, China*
[b] *Dali University, Dali, China*
[c] *Wuhu Institute of Technology, Wuhu, China*
[d] *Key Laboratory of Anhui Province for the New Technology of Chinese Medicine Decoction Pieces Manufacturing, Hefei, China*
[e] *Anhui Academy of Chinese Medicine Institute of Chinese Medicine Resources Protection and Development, Hefei, China*

ARTICLE INFO

ABSTRACT

Ethnopharmacological relevance: Fructus mume herbs have been used to convergence and antidiarrheal in clinical practice in China for thousands of years.

Aim of the study: This study aimed to investigate the molecular mechanism of Fructus mume in the treatment of UC through network pharmacology analysis and experimental validation *in vivo*.

Materials and methods: The main components of Fructus mume were initially identified with the aid of liquid chromatography-mass spectrometry. Using the network pharmacology approach, we predicted the targets of the active components and mapped target genes related to UC. We further evaluated the pharmacodynamic effects of Fructus mume on UC *in vivo* using a DSS-induced mousemodel of colitis. The degree of pathological damage in mousecolon tissue was examined via hematoxylin-eosin (HE) staining. The results of network pharmacology predictions were further verified measuring the levels of inflammatory and oxidation-related factors in mouse colon tissue via enzyme linked immunosorbent assay method and Western blot analysis.

Results: A total of 16 chemical components of Fructus mume were identified, among which 11 active components were screened based on the Ribinski rule and 368 targets predicted. KEGG pathway analysis showed that the predicted targets involved multiple signaling pathways, including PI3K-Akt, AGE-RAGE and HIF-1. In pharma-codynamic experiments, Fructus mume induced a significant increase in colon length and improved the degree of damage to colon tissue. In addition, FM inhibited the increase in TNF-α, IL-1β, NADPH and ROS levels in sera of UC mice, thereby suppressing the occurrence and development of UC. At higher concentrations, Fructus mume inhibited protein expression of downstream related (p38, p-p38, NF-kB and p-NF-kB) through regulation of the AGE/RAGE pathway, further contributing to suppression of UC in mice.

Conclusion: Our experiments provide important insights into the pharmacological basis of Fructus mume and its potential multicomponent-multitarget-multipathway pharmacological activities against UC. The therapeutic mechanism of Fructus mume may be associated with suppression of protein expression, p38, p-p38, NF-kB and p-NF-kB, in the AGE/RAGE pathway, partially validating the results from network pharmacology analysis. The collective findings provide a theoretical basis for the further development and clinical application of Fructus mume.

1. Introduction

Ulcerative colitis (UC) is a non-specific gastrointestinal inflammatory disease characterized by diarrhea, mucus, pus, and blood in the stool. The lesions are limited to the mucosa and submucosa of the large intestine (Ng et al., 2017). The specific causes of UC are yet to be established, bacteria, genetics, and intestinal flora dysregulation are proposed to serve as the main risk factors. In addition, lifestyle factors, such as a nitroso-rich diet, tobacco, and alcohol, are related to the occurrence and development of UC. Currently, the treatment of ulcerative colitis typically includes medication therapy and potential surgical intervention. Medication therapy usually involves anti-inflammatory drugs (glucocorticoids, 5-aminosalicylic acid drugs etc.), immunosuppressants (allopurinol, cyclosporine, methotrexate, and folic acid, etc.) and biologics (tumor necrosis factor α inhibitors and anti-interleukin 23 antibodies etc) to reduce inflammation and control symptoms. At present, the 5-aminosalicylic acid drugs mesalazine and sulfasalazine are the basic treatment options for UC (Hauso et al., 2015). However, it may also cause some adverse reactions, including headache, nausea, vomiting, diarrhea, rash, abnormal liver function, and kidney function abnormalities.

Traditional Chinese medicine advocates that weakness of the spleen and stomach and the evils of dampness and heat are the primary factors underlying UC. Cold and heat are the main pathological characteristics, and therefore, treatment is predominantly based on "clearing heat and removing dampness". Recent studies have reported that compared with chemical drugs, FM formulations have better therapeutic effects and fewer side effects (Zong et al., 2023). As the main medicine in prescriptions, FM is available as a medical drug or food product. Further research is required to elucidate its underlying mechanisms of action, with a view to developing safer and effective drugs for UC.

FM is the dry and immature fruit of *Prunus mume* Sieb.et Zucc. The fruit was recorded in "Shang Han Lun" to warm the internal organs, with utility as a treatment for chronic diarrhea and other symptoms based on effects such as constricting the lungs and purging the intestines, promoting the production of body fluids, and expelling roundworm (National Pharmacopoeia Commission, 2020). The chemical components of FM are classified into organic acids, flavonoids, amino acids and polysaccharides (Li et al., 2020). Modern pharmacological studies have demonstrated that FM has anti-tumor, antibacterial and anti-inflammatory properties and curative effects on UC (Zhang et al., 2017; Ma et al., 2018; Zhang et al., 2021). The FM decoction has been shown to induce significant improvement in weight loss and intestinal bleeding and increase activity of SOD in colon tissue of UC rats (He et al., 2012). However, due to the diversity of active ingredients of FM and complexity of its structure, the specific targets and mechanisms of action against UC are yet to be established.

Network pharmacology is a holistic and systematic approach. Based on the multi-component, multi-target and synergistic effects of Chinese medicine and its compounds, network pharmacology can be effectively applied to construct a multi-level network of "disease-phenotype-gene-drug". From a holistic perspective, exploring the relationship between drugs and diseases is consistent with the overall view of Chinese medicine and principles of dialectical treatment (Liu et al., 2012). Researchers using network pharmacology methods to determine the effective components and mechanisms of *Schisandra chinensis* action for treatment of asthma successfully screened eight active ingredients and key targets, such as Ptgs2 and Nos2. Schisandrol B was predicted to be the most relevant key component for asthma (Lv et al., 2020). In addition, this method was used to analyze the pharmacological active ingredients of Guanxinning tablets (GXNT), and to predict the mechanisms of action of its active ingredients, revealing the involvement of multiple pathways (MAPK, VEGF, and TNF) in anti-thrombotic activity (Wang et al., 2020).

In this study, the ultra performance liquid chromatography tandem mass spectrometry (UPLC-MS/MS) method was utilized for rapid determination of the main chemical components of FM. The TCMSP and PubChem databases were combined in network pharmacology analyses for screening of active ingredients and targets related to UC. Functional network analysis of "chemical components-disease targets" was conducted to predict the mechanisms of action of FM against UC. Experiments on a mouse UC model validated the network pharmacology results, supporting the clinical development of FM as a therapeutic agent for UC (Fig. 1).

2. Materials and methods

2.1. Materials and regents

Fructus mume (FM; College of Pharmacy, Anhui University of Chinese Medicine, AnHui, China), reference standards of benzoic acid, quercitrin, caffeic acid, fumaric acid, chlorogenic acid, protocatechuic acid, succinic acid, quinic acid, rutin, citrate, malic acid, kaempferol, ursolic acid, amygdalin, apigenin and 5-hydroxymethyl furfural were purchased from Shanghai Yuanye Biotechnology Co., Ltd(Shanghai, China). The purity of all standard ingredients was ≥ 98 %. Mesalazine (Losan Pharma GmbH Germany, Shanghai Sanwei Pharmaceutical Company, Shanghai, China), RAGE inhibitor (FPS-ZM1; Shanghai Yuanye Co., Ltd), Dextrose Sodium Sulfate (DSS; MP Company, Canada), TNF-α, IL-1β, ROS, and NADPH ELISA kits (Beijing Sizhengbai Biotechnology, Beijing, China), BCA protein quantitative kit (Thermo Fisher, USA), p38, AGEs, NF-kB, p-p38, RAGE, p-NF-kB antibody (Beijing Zhongshan Golden Bridge Company, Beijing, China), and 4 % paraformaldehyde fixative (Tianjin Solomon Biotechnology Company, Tianjin, Chian) were used for experiments in this study.

2.2. Preparation of the control sample

The appropriate amount of Benzoic acid, quercetin, caffeic acid, fumaric acid, chlorogenic acid, protocatechuic acid, succinic acid, quinic acid, rutin, citric acid, malic acid, kaempferol, ursolic acid, amygdalin, Apigenin, 5-hydroxymethyl furfural was accurately weighed using a 1/100,000 precision analytical balance (Sartorius Group, Germany) in turn. Place the samples in 25 mL volumetric flasks, add ultrapure water to prepare the controls at 0.12, 0.11, 1.21, 2.64, 1.30, 1.31, 2.40, 2.69, 1.41, 12.31, 6.12, 0.41, 2.01, 0.50, 2.58, and 0.98 mg/mL.

2.3. Preparation of FM test samples

In total, 12 batches of FM samples were collected from the regions of Sichuan and Fujian. The sample powder (1 g) was precisely weighed, placed in a 50 mL centrifuge tube, 25 mL of 80 % methanol added, and weighed. After ultrasonication for 30 min, the sample was allowed to cool, centrifuged at 12000r for 15 min, and passed through a 0.22 μm filter membrane to obtain the filtrate.

2.4. LC-MS analysis

Samples were analyzed using liquid chromatography-mass spectrometry (LC-MS) with a QUAD-4500 triple quadrupole linear ion trap mass spectrometry system (AB SCIEX, USA). The separation was performed using an Agilent ZORBAX SB-C18 column (3.0 mm × 100 mm, 3.5 μm, Agilent, USA). The column temperature was maintained at 30 °C and flow rate at 0.2 mL/min, with 0.2 % formic acid in water as mobile phase A and 0.2 % formic acid in acetonitrile as mobile phase B.

The mobile phase comprised 0.2 % formic acid–water (A) and 0.2 % acid-acetonitrile (B). A gradient elution procedure was used: 0–3 min, 10–30 % A; 3–7 min, 30–50 % A; 7–10 min, 50–80 % A; 10–14.5 min, 80–10 % A; 14.5–17 min, 10 % A. The injection volume was 1 μL and mass spectrometry detection mode was multi-reaction monitoring (MRM). The conditions included a spray voltage of 5.5 kV and an ionized
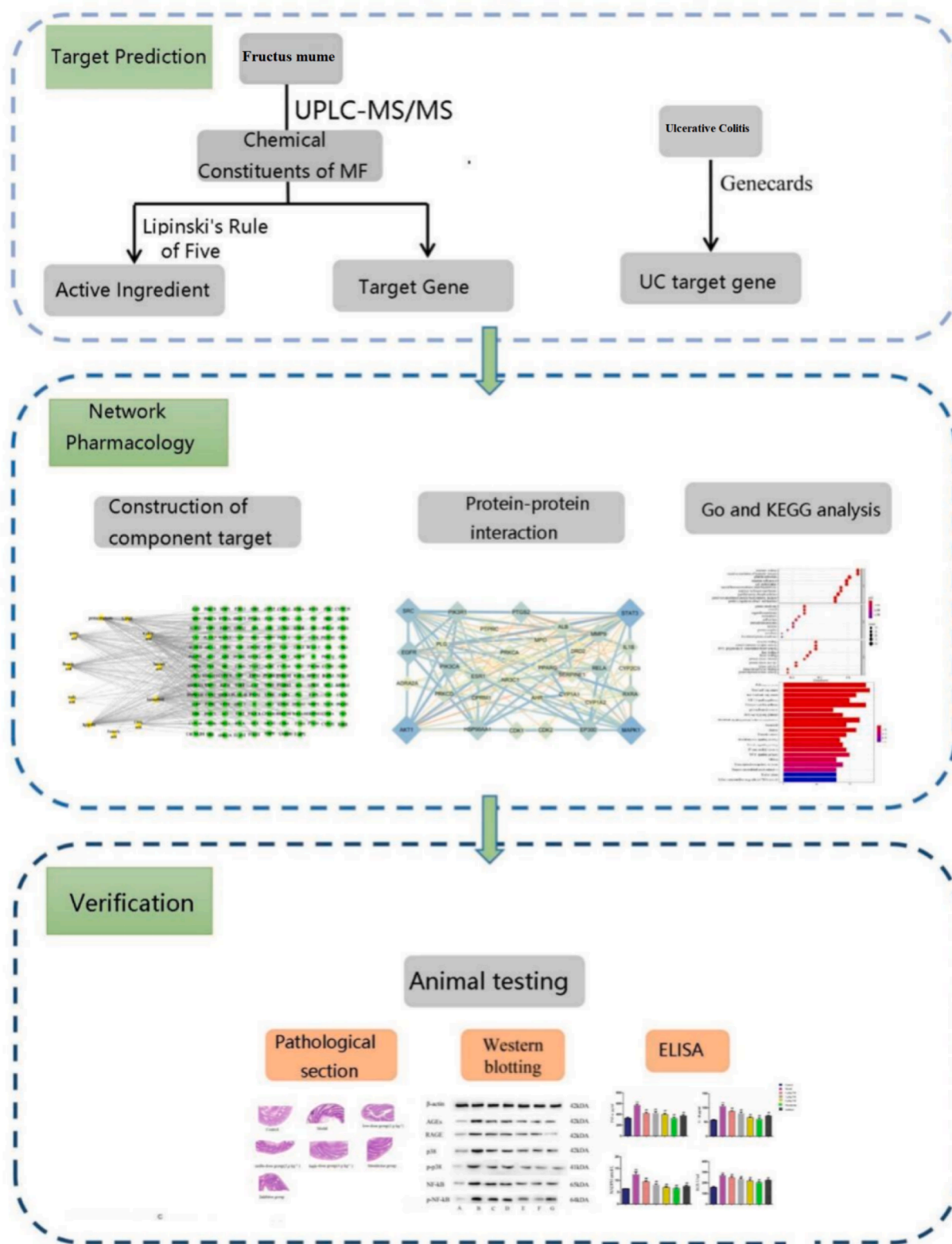
Fig. 1. Overall flowchart of this study.

temperature of 550℃. Nitrogen was used for Curtain Gas, Atomized Gas (Gas1), and Auxiliary Gas (Gas2), with pressures set at 35, 55, and 55 psi, respectively. A total of 16 components were collected using Analyst software (version 1.6). The chemical structures of the main compounds of FM were generated with ChemDraw from CambridgeSoft, which allowed for accurate mass analyses for LC/MS (electrospray), including adducts and protonated molecules.

2.5. Screening of active constituents of FM

Drug-likeness (Xu et al., 2021) refers to the possibility of chemical components becoming a drug while Lipinski's rules summarize the drug-like properties produced upon oral administration and provide a classic method for analyzing the drug-like nature of compounds. The specific screening rules for active compounds are as follows: relative molecular weight (MW) $\leq$ 500, hydrogen bond donors (the number of hydrogen atoms connected to O and N, nOHNH) $\leq$ 5, hydrogen bond receptor (the number of O and N, nON) $\leq$ 10, and lipid water partition coefficient (miLog P) $\leq$ 4.15. In cases where the above conditions are met, when these ingredients are administered orally, they have better availability in the process of biological transformation. Since FM is usually administered orally, Linpinski rules were applied to analyze the drug-like properties of the chemical components of FM and identify active ingredients.

2.6. Establishment of a SDF format file for active ingredients of FM

The molecular 2D structure of the active compound was mapped with PubChem (https: //pubchem.ncbi.nlm. nih.gov/) database and saved in the SDF format.

2.7. Prediction of potential targets for active ingredients of FM

Swiss Target Prediction (https://www.swisstargetprediction.ch/) is a web server used to accurately predict the targets of bioactive molecules based on two- and three-dimensional similarities of known ligands, which provides valuable insights into their mechanisms of action (Gfeller et al., 2014). The SDF format files of active ingredients identified via LC-MS were uploaded to the Swiss Target Prediction server and "Homo sapiens" selected as the species. The target prediction results were sorted from high to low according to "Probability **>** 0.2" and the official names of drug targets retrieved through the UniProtKB search function in the UniProt database (https://www.uniprot.org/).

2.8. Mapping of UC-related targets for active ingredients of FM

Genes potentially related to UC were searched using the keyword "Ulcerative colitis" in the GeneCards database. Comparison of the data with the targets obtained from Swiss Target Prediction server led to the identification of targets of the active ingredients in FM potentially involved in pathways affecting UC.

2.9. Construction of protein-protein and component-target networks

Targets of the active ingredients and UC were imported into the String database.

(https://string-db.org/) and the corresponding protein–protein interaction network diagrams generated. We selected 'Homo sapiens', set the interaction score to 0.700, hid the unconnected nodes, and obtained protein interaction diagrams. We used Cytoscape 3.7.1 software to combine the active ingredient targets in FM with the disease targets of UC, generated a network analysis topology map, exported the data, and calculated the median and maximum values of its degree. The median and maximum values were subsequently inputted into Cytoscape 3.7.1 software for screening and the core targets for treatment of UC obtained. The significance of each node in the network was determined by the degree of topological parameters. The degree of a node refers to the number of edges connected to that node (the higher the degree, the more nodes directly connected, and the greater importance of the node in the network). The edges represent the interactions between compounds and targets in the network.

2.10. Functional enrichment analysis of potential action targets

The Bioscape Annotation Database DAVID (https://david. ncifcrf.go v/summary. jsp) is a reliable, effective, and intuitive online bioinformatics annotation tool for understanding the biological functions of genes and protein lists on a large scale for biomedical researchers. Gene ontology (GO) enrichment and KEGG pathway annotation analyses of basic ontology terms were performed using DAVID for potential targets of FM, and P < 0.05 considered statistically significant.

2.11. UC animal experiments

2.11.1. Animal treatment and modeling

After a week of adaptive breeding, 70 specific pathogen-free (SPF) rats were randomly divided into seven groups (control, model, FM low, medium, and high groups treated with doses of (1, 2, and 4 g·kg^{-1}·d^{-1}) , Mesalazine (50 mg·kg^{-1}·d^{-1}, intraperitoneal injectio), and inhibitor (5 mg·kg^{-1}·d^{-1}, intraperitoneal injectio). The control and model groups were administered normal saline. After three days of treatment, rats in all but the control groups were switched to 3 % DSS solution for a total of 7 days. The average amount of drinking water was 5 mL per day over an experimental period of 10 days.

All animal procedures were performed according to NIH guidelines and were approved by the Ethical Committee of Anhui University of Chinese Medicine (Certificate number: 2022004).

2.11.2. Examination of in vitro characteristics

After the treatment period, weight, softness and hardness of stool and occult blood in feces of each group of rats were recorded every afternoon from 15:00 to 16:00. The disease activity index of mousewas calculated as follows:

$$DAI = (diseaseactivityindex)$$
$$= \frac{Weightlossscore + stooltraitscore + stoolbloodscore}{3}$$

2.11.3. Animal sample collection and processing

On day 10 of the experiment, rats were fasted for 24 h without water. On day 11, took blood from mouse eye balls. Blood plasma was centrifuged in a low-temperature high-speed centrifuge at 4 °C and 5000 r/min for 8 min. The supernatant was collected and stored in aliquots at −20 ℃. TNF-α, IL-1β, ROS and NADPH contents were determined according to ELISA instructions. A sample of the colon was obtained. Plasma samples were centrifuged in a high-speed low-temperature instrument at 8000 r/min at 4℃, the supernatant obtained and stored at −80℃. Colon tissue was washed with normal saline, placed in 10 times the volume of 4 % paraformaldehyde solution, and maintained at 4℃ for 24 h for fixation. A further 1.5 cm of colon tissue was obtained, sectioned, and washed with normal saline, followed by incubation in six times the volume of normal saline for homogenization for about 4 h. Samples were centrifuged for 10 min at 4 °C in a high-speed low-temperature centrifuge and the supernatant stored at − 80℃.

2.11.4. Pathological examination and HE staining of colon tissue

The mousecolon tissues of each group fixed with 4 % paraformaldehyde for 24 h were removed, washed first with water, dehydrated, soaked in wax, and finally embedded in paraffin. The tissues were routinely paraffin-cut and stained with hematoxylin-eosin (HE) for histological examination.

2.11.5. Western blot analysis

mousecolon tissue was cut into small sections and treated with 150–250 μL lysate per 20 mg tissue (protease and phosphatase inhibitors were added to lysates). Lysed samples were centrifuged at 4℃ and 12000 rpm for 15 min, the supernatant collected, and protein concentrations determined using the BCA method. Protein samples were boiled

for 5–10 min for denaturation, separated using a 12 % SDS-polyacrylamide gel, and transferred to PVDF membrane. The membrane was blocked with 5 % skimmed milk for 2 h and incubated with primary antibodies against p38, p-p38, AGEs, RAGE, NF-kB, p-NF-kB and β-actin at 4℃ overnight. Subsequently, the membrane was washed three times with TBST for 10 min each time and incubated with the corresponding secondary antibody for 1 h at room temperature. The gray value was visually analyzed with ECL developer and a chemometric gel imaging system.

2.12. Statistical analysis

Each experiment was repeated at least three times. All data were statistically analyzed using SPSS 22.0 software and expressed as mean ± standard error ($\overline{X} \pm$ SEM). Data were considered statistically significant at $P < 0.05$.

3. Results

3.1. Optimization of sample preparation

Ultrasonic extraction of FM is reported to be more effective than refluxing (Li et al., 2020). To determine the best extraction conditions, based on previous findings (Ou et al., 2020), three factors were selected and the properties of each component optimized. The effects of extraction solvent (water, 50 % methanol, 80 % methanol), ratio of solvent to sample (15:1, 25:1 and 35:1) and ultrasonic time (20, 30 and 40 min) on extraction efficiency were examined. Our results showed optimal extraction efficiency at a concentration of 80 % methanol, solvent to sample ratio of 25:1 and ultrasonic time of 30 min.

3.2. Optimization of MS and LC conditions

Various chromatographic conditions, such as column type, mobile phase composition and pH, were examined in preliminary experiments to obtain the ideal chromatographic profile and optimize retention time and peak shape. Two column types were compared, specifically, BEH C18 (100 mm × 2.1 mm, 1.7 μm) and ZORBAX SB-C18 (3.0 mm × 100 mm, 3.5 μm), to optimize retention time of the target analyte. The results showed that under the same conditions, the ZORBAX SB-C18 column had strong retention capacity, good resolution, and short analysis time for all analytes. Acetonitrile, a polar aprotic solvent with better elution capacity, separation selectivity and peak shape than methanol, was selected as the organic solvent for the mobile phase. According to earlier studies, mixed solution containing formic acid as a mobile phase additive could increase sensitivity and improve the peak shape of the measured components. Therefore, acetonitrile-0.1 % formic acid water, 0.1 % acetonitrile-0.1 % formic acid water and 0.2 % acetonitrile-0.2 % formic acid water mixtures were compared in this study. Notably, the 0.2 % acetonitrile-0.2 % formic acid water combination produced the optimal peak in the shortest time.

Full-scan MS was conducted to assess the target compounds in positive and negative modes for determining optimal MS conditions. The sensitivity and intensity of ursolic acid, amygdalin, apigenin and 5-hydroxymethylfurfural standards in the positive mode were higher than those in the negative mode but better for the other standards in the negative mode. The MRM chromatograms of 16 standards are depicted in Fig. S1(A).

3.3. Identification of active ingredients in FM

Mass spectrometry information on materials obtained from the experiment was compared with related literature reports. Consequently, 16 compounds were identified in FM, of which were validated based on reference standards. The results are summarized in Table S1. Mass spectra and structures of each compound are shown in Fig. S1(B).

3.4. Content quantification of the 16 main active ingredients of FM

We obtained 1 μL standard and mixed standard stock solutions of different concentrations, which were subjected to stepwise dilution. Experiments were performed in parallel three times. A standard curve with mass concentration X (μg/mL) as the abscissa and peak area (y) as the ordinate is presented in Table S1. Each sample solution was assessed, the 16 compounds quantified based on the corresponding standard curves (Table S1), and changes in quantity evaluated (Table S2). The compounds assessed included 10 organic acids, 4 flavonoids, amygdalin and 5-hydroxymethylfurfural. We observed a number of differences in composition and organic acid contents among the samples. The citric acid content was between 13.28 % and 16.85 %, which was higher than the pharmacopoeia standard (content of no less than 12 %). Malic acid, fumaric acid, quinic acid and succinic acid levels were the second highest while those of protocatechuic acid and benzoic acid were much lower. Among the flavonoids, the apigenin content was the highest while that of quercitrin was the lowest. The contents of amygdalin and 5-hydroxymethylfurfural were 1.59 % and 1.60 %, respectively.

3.5. Determination of the potential main active ingredients of FM

The 16 components determined via LC-MS/MS were screened for classification as active ingredients based on the Lipinski rules. The results are listed in Table 1.

### 3.6. Screening the targets of Anti-UC active components of FM

The 2D.SDF structures of the 11 compounds mentioned above were queried using the PubChem database and imported into the SwissTarget Prediction platform, from which 368 corresponding targets were obtained. A total of 1977 UC-related targets were obtained by querying GeneCards. The selected drug and disease targets were inputted into the Venn diagram production software Venny 2.1. Overall, 151 common targets were mapped, as shown in Fig. 2A.

3.7. PPI network construction and analysis

The common targets of drugs and diseases were imported into the String database (https://string-db.org/cgi/input.pl) to construct the PPI network (Fig. 2B). Customized interaction network confidence was 0.990 and data were exported using Cytoscape3.7.1 software. The NetworkAnalyzer tool was employed to perform topology analysis and a core PPI network diagram generated with the two parameters of degree and betweenness centrality as reference standards (Fig. 2C). The results support the involvement of key proteins, such as signal transducer and activator of transcription 3 (STAT3), matrix metalloproteinase 9 (MMP9) and serine/threonine protein kinase 1 (protein kinase Bα,

Table 1
Potential Main Active Components of FM.

Compound	MW	miLog P	nOHNH	Non
benzoic acid	122.12	1.85	1	2
caffeic acid	180.16	0.94	3	4
fumaric acid	116.07	−0.68	2	4
protocatechuic acid	154.02	0.88	3	4
succinic acid	118.09	−0.66	2	4
quinic acid	192.17	−2.33	5	6
citric acid	192.12	−1.98	4	7
malic acid	134.09	−1.57	3	5
kaempferol	286.24	2.17	4	6
apigenin	270.24	2.46	3	5
5-hydroxymethyl furfural	126.11	0.56	1	3
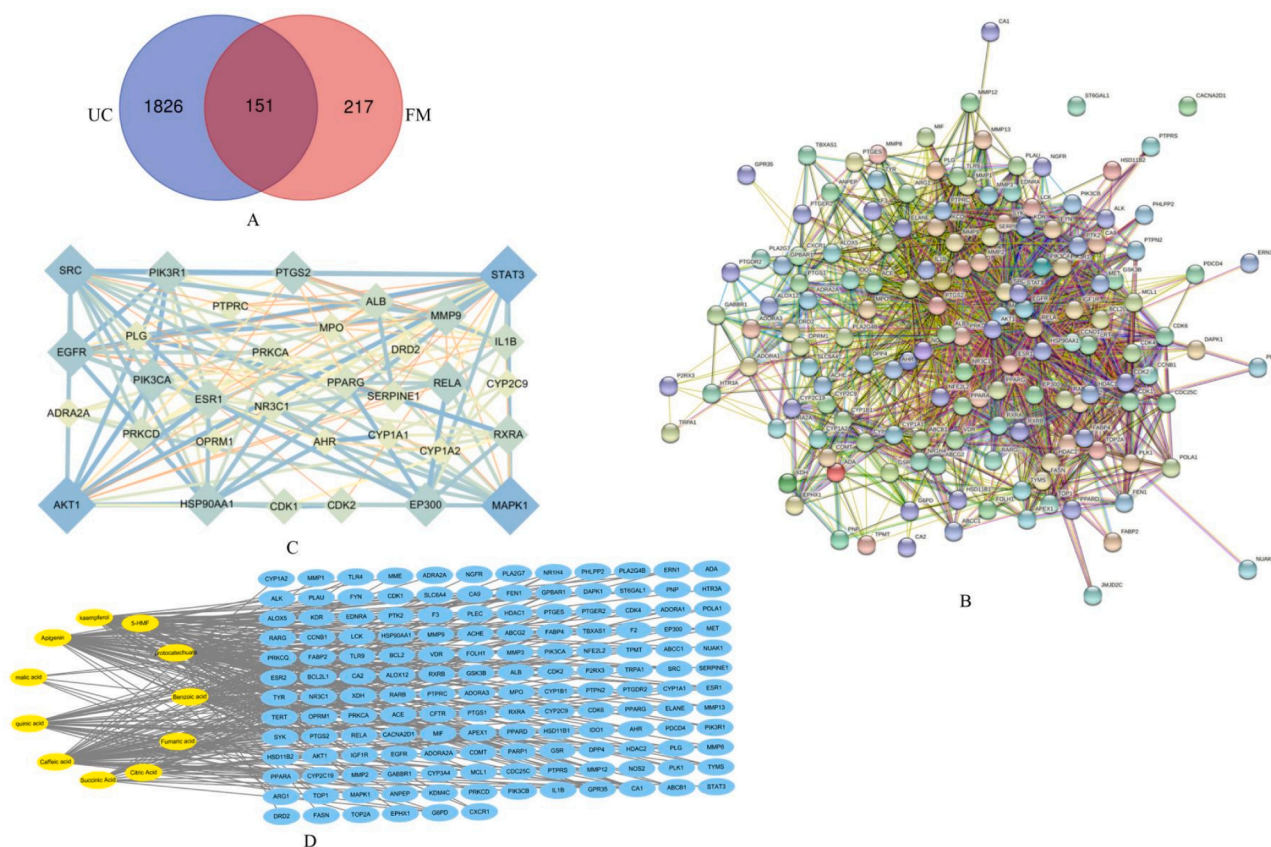
Fig. 2. Construction of FM active ingredient—target gene network in UC and screening of key molecules. **(A)** Screening of targets for the main active components of FM on UC. 217 Predicted targets (in the pink circle) were mapped to 1826 UC-related targets (in the blue circle).The intersection of these targets resulted in a total of 151 potential targets for treatment of UC. **(B)** PPI network of related targets of FM in the treatment of UC. **(C)**PPI network of core targets of FM in the treatment of UC. **(D)** "Active ingredient-target" network diagram of FM.

AKT1), in FM activity against UC. STAT3 plays an important role in UC as it is involved in regulating inflammatory responses. Studies have shown that the expression levels of STAT3 in the intestinal tissues of patients with UC are significantly increased. Therefore, inhibiting the activity of STAT3 may help alleviate the symptoms of UC. Additionally, MMP9 is also involved in the development of UC. Research has indicated that the expression levels of MMP9 in the intestinal tissues of UC patients are significantly increased. MMP9 can degrade the matrix molecules in intestinal tissues, leading to tissue damage and ulcer formation.

3.8. Construction of a component–target network

An active component–target network of FM for UC was constructed using Cytoscape 3.7.1 software. Network topology analysis showed that the degree and betweenness centrality of caffeic acid were the highest (degree = 57, betweenness centrality = 0.36787426). The degree and betweenness centrality of CA1, a target of FM components, also ranked among the top (degree = 10, betweenness centrality = 0.07807696) ; Fig. 2**D**. Our results showed that multiple targets were associated with multiple components, suggesting that different components of FM exert synergistic effects leading to greater therapeutic efficacy.

3.9. GO enrichment and KEGG pathway enrichment analysis

GO enrichment analysis is subdivided into three ontologies: 1. Biological Process (BP), 2. Molecular Function (MF), and 3. Cellular Component (CC). Using DAVID database, GO enrichment analysis was conducted on 151 potential targets of FM against UC, with statistical significance set at $P < 0.05$. A total of 206 biological processes or

pathways were obtained, among which 80 were related to BP, 76 to MF, and 50 to CC. According to P values sorted from small to large, the top 10 were selected and R language used to generate a high-level bubble chart, as shown in Fig. 3**A**. The bubble represents the number of genes enriched in GO entry, i.e., the larger the bubble, the greater number of genes enriched. The targets mainly involved response to drug, plasma membrane, and enzyme binding.The common targets were subjected to KEGG pathway enrichment analysis and screened according to P value ≤ 0.05. Overall, 97 signaling pathways were enriched. R 3.6.3 was used and the clusterProfiler package installed and quoted. The first 20 channels were selected to generate a histogram (Fig. 3**B**), including Pathways in cancer, Small cell lung cancer, Non-small cell lung cancer, etc. Among these, AGEs and their receptors (RAGE) exist on the surface of many cell types. The Interactions of AGE and RAGE trigger activation of intracellular oxidative stress, PIK3-AKT1 and Jak-STAT signals, thereby producing a large number of growth factors and pro-inflammatory cytokines, such as IL-1βa, IL-6 and NF-κB, which could promote the development of UC. The specific signaling pathways are shown in Fig. 3**C** (This image is from DAVID's database). The activation of the AGE-RAGE signaling pathway can trigger inflammatory responses, including the promotion of inflammatory cell infiltration and the release of inflammatory factors, leading to tissue damage and the development of inflammatory diseases. Furthermore, activation of the AGE-RAGE signaling pathway can also lead to increased intracellular oxidative stress, thereby affecting normal cellular function, accelerating cellular aging, and the progression of diseases. The AGE-RAGE signaling pathway plays a significant role in physiological and pathological processes such as inflammation and oxidative stress, and may have potential implications for the development of UC.
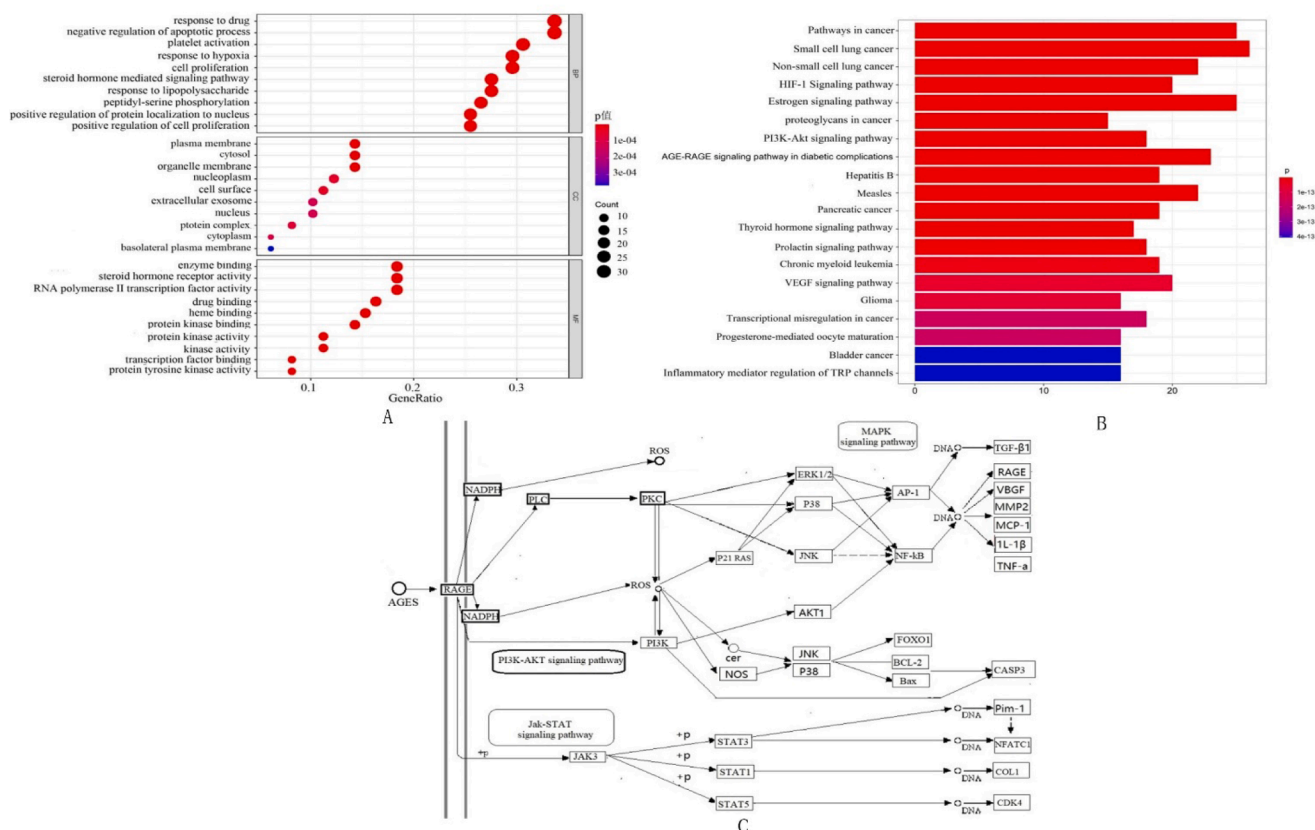
Fig. 3. (A)Enrichment analysis results; (B)KEGG pathway enrichment analysis; (C)AGEs-RAGE signaling pathway map.

3.10. General indicators of FM activity in DSS-induced UC rats

On day 3 after modeling, animals from the model group and each treatment group experienced weight loss, dull coat color, reduced food intake, and varying degrees of diarrhea. Weight loss of the model group was the fastest, with evidence of hematochezia. Body mass, hair and activity levels were all normal.Compared with the control group, disease activity score (DAI) of the model group was significantly higher (P < 0.01). Relative to the model group, DAI scores of rats in FM administration groups were significantly lower (P < 0.05). The scores of the mesalazine and inhibitor groups were markedly decreased (P < 0.01 and P < 0.05, respectively) compared to the model group, as shown in Table 2. Our results showed that all treatments effectively reduced the DAI scores representative of symptoms of UC rats.

3.11. Effect of FM on colon length

The mousecolon lengths from each experimental group are presented in Fig. 4**A.** Colon length of the model group was significantly smaller than that of the control group (P < 0.01), indicating successful generation of the UC model. Compared with the model group, colon lengths of

Table 2
Disease activity score of mice in each group ($\overline{X} \pm s$).

Group	Score
Control	0
Model	8.56 ± 0.12**
Low-dose group	6.39 ± 0.45##
Middle-dose group	5.76 ± 0.19##
High-dose group	3.74 ± 0.24##
The mesalazine group	1.87 ± 0.31##
The inhibitor group	3.17 ± 0.41##

** P < 0.01 vs normal group; ## P < 0.01 vs model group.

the FM, mesalazine and inhibitor groups were significantly increased (P < 0.01), clearly demonstrating FM-induced improvement of UC.

3.12. Effect of FM on microscopic injury of colon

The results of HE staining are illustrated in Fig. 5. In the control group, colon tissue structure was complete, glands were arranged neatly, and no ulcers were detected. In the model group, obvious diseased tissue was present in colon and the upper mucosal cells were shed and necrotic. Part of the colon tissue in the low-dose FM group was severely damaged, with infiltration of inflammatory cells. The medium-dose group showed less colonic tissue damage and ordered arrangement of some glands, with a limited number of inflammatory cells. The colon tissue in the high-dose group displayed only a small amount of damage. The majority of glands were arranged neatly and part of the tissue structure was complete. In the mesalazine group, villi of the colon tissue were clear and mucosa was not damaged or ulcerated. In the inhibitor group, colon tissue was relatively complete with limited inflammatory cell infiltration. All animals in the treatment groups showed improvement of UC.

3.13. Effects of FM on expression of TNF-α, IL-1β, NADPH and ROS

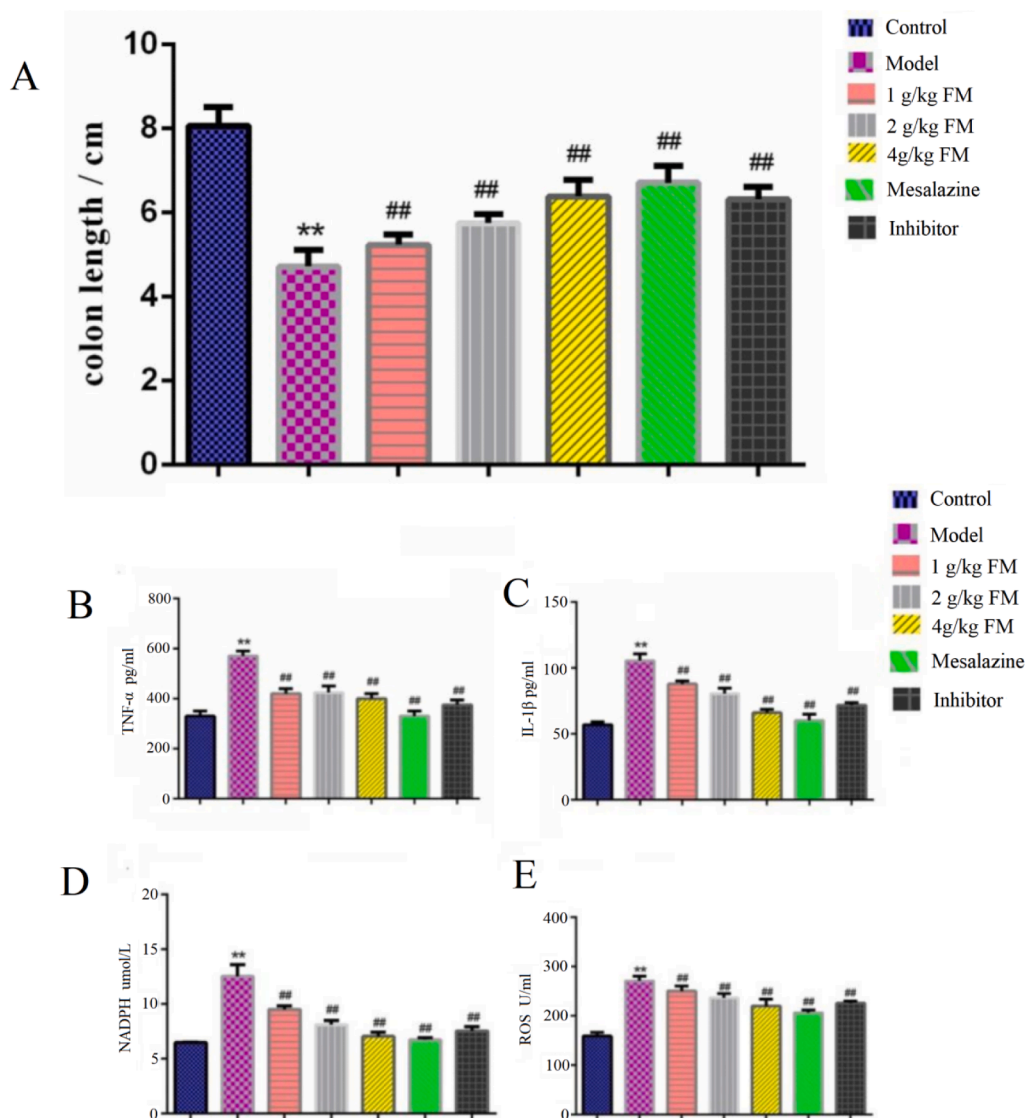ELISA was applied to determine the levels of TNF-α, IL-1β, NADPH and ROS in sera of mice. The levels of inflammatory factors (TNF-α, IL-1β), reduced coenzymes (NADPH) and reactive oxygen species (ROS) were significantly higher relative to the control group, clearly supporting successful generation of the UC model (Fig. 4B. Fig. 4C. Fig. 4D). Compared with the model group, levels of TNF-α, IL-1β, and ROS in sera of mice from each FM treatment group were significantly reduced (P < 0.05). In view of these findings, we propose that FM suppresses the generation of TNF-α, IL-1β, NADPH and ROS levels in mice with DSS-induced UC, thereby inhibiting the occurrence and development of UC.

Fig. 4. (A) Effect of FM on the length of colons were observed after FM administration (1, 2, and 4 g/kg), Mesalazine(50 mg/kg) and Inhibitor(5 mg/kg). Data were expressed as the mean ± SEM. **P < 0.01 vs control group; ##P < 0.01 vs model group. **(B)** Effect of FM on TNF-α. **(C)** Effect of FM on IL-1β. **(D)** Effect of FM on NADPH. **(E)** Effect of FM on ROS.

3.14. Effects of FM on proteins related to AGE-RAGE signaling

We observed changes in the levels of AGE, RAGE, p38, p-p38,NF-kB and p-NF-kB proteins involved in the AGE-RAGE signaling pathway in each group. The levels of AGE, RAGE, p38, p-p38, NF-kB and p-NF-kB proteins were significantly increased in the model group compared with the control group (P < 0.01; P < 0.05), as shown in Fig. 6A. Notably, relative to the model group, expression levels of each protein in the FM, mesalazine and inhibitor treatment groups were markedly reduced (P < 0.05). The gray value of protein expression in each group showed similar trends. The results are presented in Fig. 6B. Compared with the control group, expression of AGE, RAGE, p38, p-p38, NF-kB and p-NF-kB proteins in the model group was significantly higher. The levels of the corresponding proteins in the other treatment groups were significantly lower than those of the model group (P < 0.05). Based on these results, we propose that FM participates in regulation of AGE/RAGE pathway. Moreover, with increasing treatment concentrations, mRNA and protein expression levels of downstream related genes (p38, p-p38, NF-kB and p-NF-kB) were inhibited, contributing to protective effects against DSS-induced UC.

4. Discussion

In our study, 11 out of 16 components of FM were determined as active constituents via LC-MS/MS combined with database analysis. Generally, the majority of compounds show response in both the positive and negative modes although the negative ion mode has a slightly higher response, mainly since FM contains more organic acids which makes it easier to provide protons in the negative mode (Li et al., 2020). The 11 compounds displayed high contents of benzoic acid, caffeic acid, fumaric acid, protocatechuic acid, succinic acid, quinic acid, citric acid and malic acid. Organic acids may serve as the main contributors to the antioxidant activity of FM (Li et al., 2017). In the process of liver disease treatment, FM may achieve the purpose of treatment by removing peroxynitrite and reducing peroxidation. (Song et al., 2012). In an earlier study, FM extract inhibited ROS production in colon tissues of mice with UC that led to significant relief of oxidative stress, thereby reducing the development of inflammation, which may be closely associated with its phenol and flavonoid contents (Seung et al., 2017). Accordingly, we propose that multiple active compounds of FM cooperatively exert their therapeutic effects.
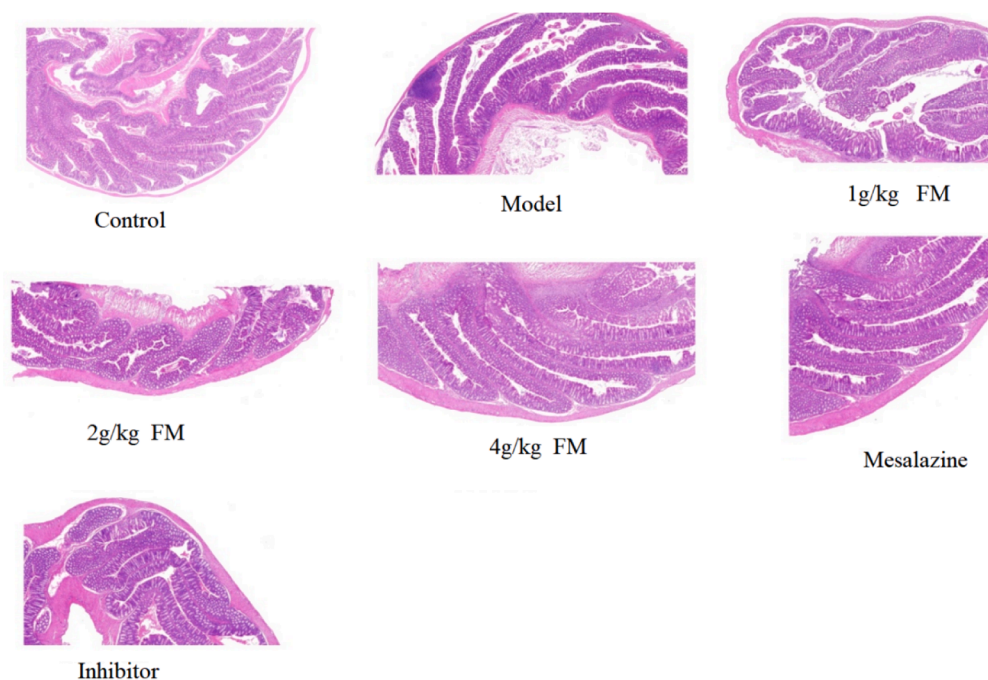
Fig. 5. Effect of FM on colonic histopathological changes in UC mice (HE staining).

To clarify the mechanism of action of FM against UC, network pharmacology was employed for further analysis. The results showed that the 11 components are closely related to 368 targets, of which 151 potential anti-UC targets were obtained through functional enrichment analysis, involving PI3K-Akt, AGE-RAGE and HIF-1 pathways (Bai et al., 2021; M et al., 2019; Kim et al., 2018a). AGE-RAGE as a pathway in inflammatory disease and involvement of RAGE ligand as an inflammatory central activator have been recently confirmed (M et al., 2019). AGE and their receptors exist on the surface of several cell types. AGE-RAGE interactions have been shown to activate intracellular oxidative stress, PIK3-AKT1 and Jak-STAT signaling channels and high expression of a number of growth factors and pro-inflammatory cytokines, including IL-1β, IL-6 and NF-κB, thereby aggravating the development of ulcerative colitis. During inflammation and oxidative stress, RAGE ligands are produced in the body and activate downstream factors, such as p38, NF-kB, TNF-α, and NADPH, exacerbating inflammation and colon tissue damage (Geetha et al., 2010). RAGE is proposed to participate in the continuation of inflammation and immune response in chronic inflammatory diseases and the pathological process (Jia et al., 2019). Recent research indicates that the AGE-RAGE signaling pathway may hold promise for treating inflammatory bowel disease (Duan et al., 2023; Zhang et al., 2023). Therefore, AGE-RAGE presents a critical pathway for therapeutic intervention in UC.

We further employed a DSS-induced mouse UC model to elucidate the mechanism of action of FM *in vivo*. The length of colon in mice with colitis was significantly shortened and the surface of colon tissue showed obvious lesions. Administration of FM led to a significant increase in colon length and improved damage to colon tissue. In addition, FM exerted suppressive effects on TNF-α, IL-1β, NADPH and ROS levels in serum of UC mice, which, in turn, inhibited the occurrence and development of UC. In addition, treatment with increasing concentrations of FM inhibited expression of downstream related p38, p-p38, NF-kB and p-NF-kB proteins via modulatory effects on the AGE/RAGE pathway.

Inflammation is an important pathological response in the pathogenesis of UC. Cytokines are the main participants in the inflammatory response and imbalance between pro-inflammatory and anti-inflammatory factors is the pathological basis for intestinal inflammation (Hao et al., 2020). TNF-α, IL-1β, NADPH and ROS are known pro-inflammatory factors. TNF-α is highly expressed in UC patients and positively correlated with severity of UC (Tang et al., 2020). IL-1β is produced by monocytes and macrophages (Kim et al., 2018b). IL-1β serves as a target for the treatment of systemic and local inflammatory diseases and therapeutic effects can be achieved by reducing its activity (Fabiani et al., 2017). Activated NADPH oxidase acts as an intracellular and extracellular electron transfer body, which converts superoxide anions into H_2O_2 and hydroxide after receiving oxygen, both of which generate reactive oxygen species (ROS) intermediate products (Gabriella et al., 2019). ROS metabolites are mainly produced in cells as a result of NADPH oxidase activity in the colonic epithelium. ROS are significantly increased in UC and directly cause oxidation in the body, damage to colon tissues and cells, and generate a repetitive chain reaction (Jiamei et al., 2018). In our experiments, FM inhibited the increase in TNF-α, IL-1β, NADPH and ROS levels in serum of UC mice, clearly indicating therapeutic effects against intestinal inflammation and inflammatory damage.

The p38 signaling pathway mediates cellular responses, such as inflammation and stress. After phosphorylation-mediated activation of p38MAPK, downstream transcription factors are regulated, promoting the secretion of IL-1, TNF-α and other cytokines, thereby causing intestinal mucosal barrier inflammation (Sánchez-Fidalgo et al., 2015). NF-κB is a key factor in this pathway, and its subunit, NF-κB p65, which is highly expressed in colonic mucosa of patients with UC, acts to destroy the physiological barrier of the mucosa, leading to increased colonic permeability and progression of UC (Amir et al., 2019). In an earlier report, Huangqin Decoction was shown to inhibit the NF-κB p65 pathway and suppress expression of nitric oxide, IL-6 and TNF-α, thereby achieving a therapeutic effect against UC (Wang et al., 2015). In this study, expression of RAGE protein in colon tissue was increased significantly with progressively higher concentrations of FM decoction. After treatment with FM or inhibitor, expression levels of AGE and RAGE proteins were decreased. The downstream related genes, p38, p-p38, NF-kB and p-NF-kB, were inhibited by these agents via regulation of the AGE/RAGE pathway, resulting in improvement of DSS-induced UC in mice. Our collective findings clearly indicate that FM significantly improves inflammation of intestinal tissues and achieves therapeutic efficacy against UC through inhibition of the AGE-RAGE pathway.
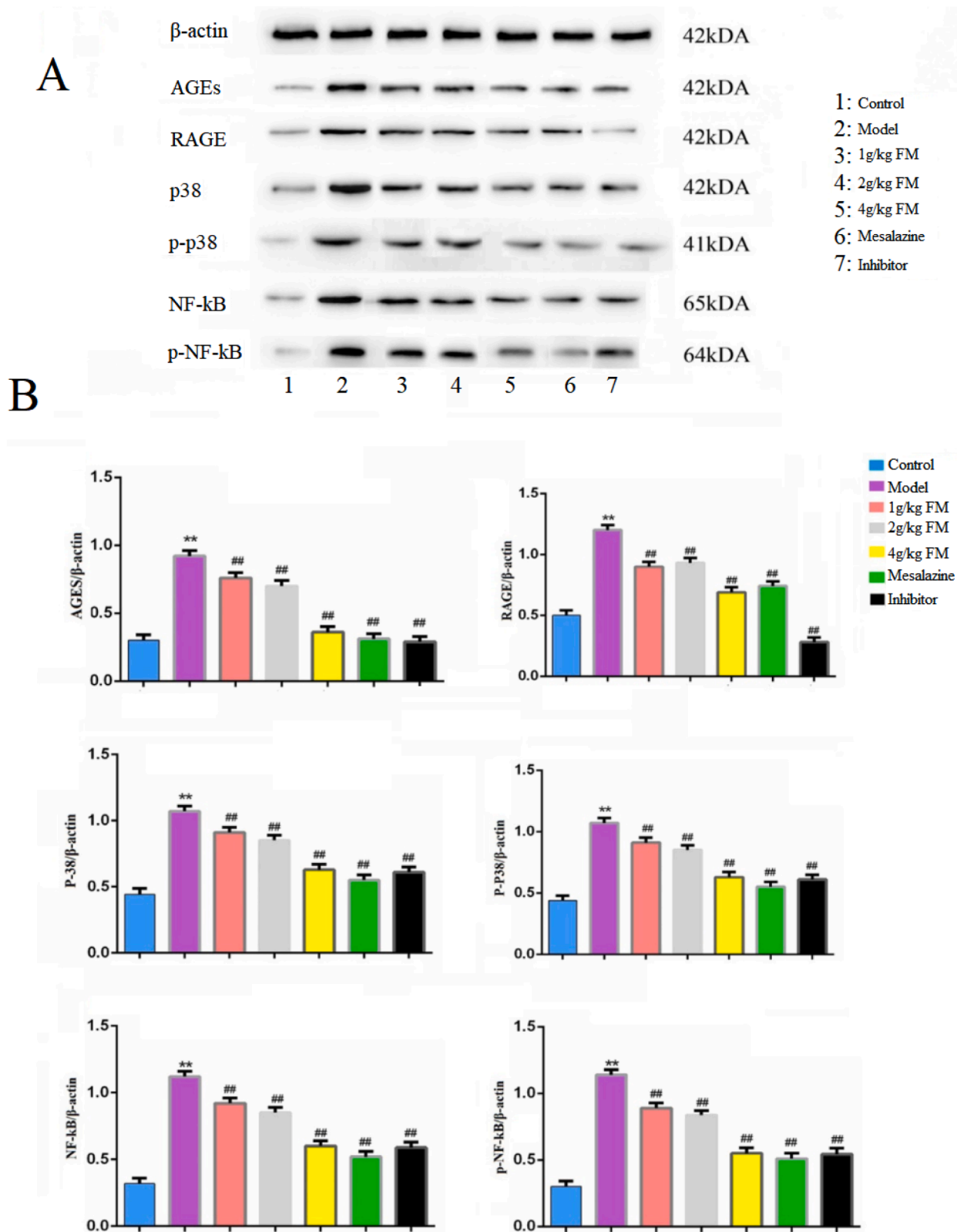
Fig. 6. A:Electrophoresis of protein expression in mouse colon. (1: Control; 2: Model; 3: 1 g/kg FM; 4: 2 g/kg FM; 5 4 g/kg FM; 6: The mesalazine group; 7: The inhibitor group); **B** Effects of FM on the expressions of AGEs、RAGE、p38、p-p38、NF-kB and p-NF-kB proteins in colon. The expressions of AGEs, RAGE, p38, p-p38, NF-kB and p-NF-kB proteins in colon were determined by western blotting analysis after FM administration (1, 2, and 4 g/kg), Mesalazine(50 mg/kg) and Inhibitor(5 mg/ml). Data were expressed as the mean $\pm$ SEM.**$P < 0.01$ vs normal group; $^{##}P < 0.01$ vs model group.

5. Conclusion

In conclusion, 11 active ingredients of FM were identified and therapeutic effects against UC clearly demonstrated. Using the network pharmacology approach, 97 signaling pathways were predicted to be associated with UC (including PI3K-Akt, AGE-RAGE and HIF-1) and the involvement of AGE-RAGE in UC further validated. The collective results provide a reference for further investigation of the pathways underlying FM inhibits DSS-induced UC and validate the utility of the network pharmacology method in accurately predicting the mechanisms of action of traditional Chinese medicines containing complex components.

Author contributions

JO and RW conceived the research ideas. RW and XW designed the experiments in detail and advised on data collection. All authors significantly contributed to the manuscript and have read and approved the final manuscript.

Funding

Declaration of competing interest

The authors declare that they have no known competing financial interests or personal relationships that could have appeared to influence the work reported in this paper.

Appendix A. Supplementary material

Supplementary data to this article can be found online at https://doi.org/10.1016/j.arabjc.2023.105534.

References

Amir, R., Asma, R., Alireza, A., 2019. Dapsone reduced acetic acid-induced inflammatory response in mousecolon tissue through inhibition of NF-kB signaling pathway. Immunopharm. Immunotoxic. 6, 635.

Bai, Y., Wang, L.L., An, J., 2021. Correlation between KRAS, NRAS, BRAF, PIK3CA gene mutations and clinicopathological features and expression of MMR protein and p53 protein in colorectal cancer tissues. J. Diagn. Path. 28(03), 183-188+193.

Body-Malapel, M., Djouina, M., 2019. The RAGE signaling pathway is involved in intestinal inflammation and represents a promising therapeutic target for Inflammatory Bowel Diseases. Mucosal Immunol. 11, 960.

Duan, Z.L , Wang Y.J., Lu, Z.H., 2023. Wumei Wan attenuates angiogenesis and inflammation by modulating RAGE signaling pathway in IBD: Network pharmacology analysis and experimental evidence[J]. Phytomedicine,111.154658-154658.

Fabiani, C., Sota, J., Tosi, G.M., 2017. The emerging role of interleukin (IL)-1 in the pathogenesis and treatment of inflammatory and degenerative eye diseases. Clin. Rheumat. 10, 3527.

Gabriella, A., Ashish, K.S., 2019. Colitis susceptibility in mice with reactive oxygen species deficiency is mediated by mucus barrier and immune defense defects. Mucosal Immunol. 11, 1385.

Geetha, S., Jonamani, N., Bernd, W., 2010. Carboxylated N-glycans on RAGE promote S100A12 binding and signaling. J. Cell Biochem. 110 (3), 645–649.

Gfeller, D., Grosdidier, A., Wirth, M., Daina, A., Michielin, O., Zoete, V., 2014. Swiss Target Prediction: a web server for target prediction of bioactive small molecules. Nucleic Acids Res. 42, W32–W38.

Hao, Y.W., Zhang, Y., Zhou, X.L., Yu, J., 2020. Based on mTOR/p-S6K1 to explore the effect mechanism of Jiawei Fuzi Lizhong Decoction on the intestinal mucosal inflammation in UC rats. Chin. J. Exp. Pharm. 13, 59–65.

Hauso, O., Martinsen, T.C., Waldum, H., 2015. 5-Aminosalicylic acid, a specific drug for ulcerative colitis. Scand. J. Gastroentero. 50 (8), 933–941.

He, A.M., Wang, Y.L., Lin, S.M., 2012. The effect of Fructus Mume decoction on rat with experimental ulcerative colitis. J. Pharm. Pract. 30 (05), 357–360.

Jiafeng, W., Yan, Z., Yulan, Z., 2019. Promoter methylation cooperates with SNPs to modulate RAGE transcription and alter UC risk. Biochem. Biophy. Rep. 17, 17–22.

Jiamei, M., 2018. Casticin prevents DSS induced ulcerative colitis in mice through inhibitions of NF-κB pathway and ROS signaling. Phytoth. Res. 10, 6108.

Kim, Y., Lee, M., Gu, H., 2018a. Hypoxia-inducible factor-1 (HIF-1) activation in myeloid cells accelerates DSS-induced colitis progression in mice. Disea Mod. Mechan. 11, 127–134.

Kim, Y., Lim, H.J., Jang, H., 2018b. Portulaca oleracea extracts and their active compounds ameliorate inflammatory bowel diseases in vitro and in vivo by modulating TNF-α, IL-6 and IL-1β signalling. Food Res. Int. 12, 058.

Li, X., Wang, R., Li, X.L., Zhang, W., Ou, J.M., 2020. UPLC feature map and pattern recognition of different processing methods of Fructus Mume. Chin. J. Tradit. Chin. Med. 11, 76–81.

Liu, Z. H., Sun, K., Wang, L., Q., 2012. Network Pharmacology: A New Opportunity for the Modernization of Traditional Chinese Medicine. Acta Pharm. Sin. 8(09), 696-703.

Lv, X., Xu, Z.Y., Xu, G.Y., Li, H., Wang, C., Chen, J.G., Sun, J.H., 2020. Investigation of the active components and mechanisms of Schisandra chinensis in the treatment of asthma based on a network pharmacology approach and experimental validation. Food Funct. 4, 2767–2773.

Ma, C., Luo, M., Y, X., Jiao, W. C., Gu., X. L., 2018. Research progress on the chemical composition and application of Fructus Mume. Sci Tech. Food Ind. 39(04), 337-341+352.

National Pharmacopoeia Commission. 2020. Pharmacopoeia of the People's Republic of China. Beijing Chin Med Sci and Tech Press, 79.

Ng, S.C., Shi, H.Y., Hamidi, N., Tang, W., 2017. Worldwide incidence and prevalence of inflammatory bowel disease in the 21st century: a systematic review of population-based studies. Lancet 152, S970–S971.

Ou, J.M., Wang, R., Li, X.L., 2020. Comparative analysis of free amino acids and nucleosides in different varieties of Mume Fructus based on simultaneous determination and multivariate statistical analyses. Int. J. Anal. Chem. 2020, 2020.

Sánchez-Fidalgo, S., Villegas, I., Rosillo, M.Á., 2015. Dietary squalene supplementation improves DSS-induced acute colitis by downregulating p38 MAPK and NFkB signaling pathways. Mol. Nutr. Food Res. 2, 518.

Seung, Y.L., Seung, J., 2017. Effects of Prunus mume Sieb. et Zucc. extract and its biopolymer encapsulation on a mouse model of colitis. J. Sci. Food Agricul. 2, 7790.

Song, Z.Y., Zhang, Q., 2012. Research on the mechanism of rhubarb and Fructus plum in the treatment of liver failure. J. Int. Tradi. Chin. West Med. 22 (04), 253–256.

Tang, X., Huang, G., Zhang, T., 2020. Elucidation of colon-protective efficacy of diosgenin in experimental TNBS-induced colitis: inhibition of NF-κB/IkB-α and Bax/Caspase-1 signaling pathways. Biosci. Biotech. Biochem. 9, 1–10.

Wang, M.L., Yang, Q.Q., Ying, X.H., Wu, Y.S., 2020. Network pharmacology-based approach uncovers the mechanism of GuanXinNing tablet for treating thrombus by MAPKs signal pathway. Front. Pharmacol. 11, 652–660.

Wang, Y.W., Zhang, H.H., Wang, Y.L., 2015. Study on the regulation of Huangqin decoction on NF-κB p65 in rats with ulcerative colitis. Acta Pharma. Sin. 1, 21–27.

Xu, J.L., Xu, Y.C., Zhu, Y., 2021. Molecular targets and associated signaling pathways of Jingshu granules in ovarian cysts based on systemic pharmacological analysis. BioMed Res. Int. 3, 321–330.

Zhang, X.Y., Xiao, H,J ,Fu, S.J., 2023. Investigate the genetic mechanisms of diabetic kidney disease complicated with inflammatory bowel disease through data mining and bioinformatic analysis [J]. Frontiers in Endocrinology,13. 1081747.

Zhang, H.Y., Li, Q., Fu, X.L., 2017. Research progress on the chemical constituents and pharmacological effects of Fructus Mume. Shanghai J. Trad. Chin. Med. S1, 296–300.

Zhang, J.C., Liang, H., Wang, Y., Xi, W., Li, Z.G., 2021. Research Progress on pharmacological action of Fructus Mume. J. Liaoning Univ. Tradi. Chin. Med. 23 (08), 122–126.

Zong, Y.C., Meng J., Mao T. Y, H., Q., Zhang P., Shi L. 2023. Repairing the intestinal mucosal barrier of traditional Chinese medicine for ulcerative colitis: a review. 14. 1273407-1273407.